

Measurements of $\nu_\mu N$ and $\bar{\nu}_\mu N$ Charged-Current Total Cross Sections

B. C. Barish, J. F. Bartlett, A. Bodek,^(a) K. W. Brown, D. Buchholz,^(b) Y. K. Chu
F. Sciulli, E. Siskind, and L. Stutte^(c)

California Institute of Technology, Pasadena, California 91125

and

H. E. Fisk, G. Krafczyk, and D. Nease

Fermi National Accelerator Laboratory, Batavia, Illinois 60510

and

O. Fackler

Rockefeller University, New York, New York 10021

(Received 14 October 1977)

Measurements of flux-normalized neutrino and antineutrino total charged-current cross sections (σ) in the energy range $45 < E < 205$ GeV are presented. We see no evidence for the anomalous sharp rise in $\sigma_{\bar{\nu}}/\sigma_\nu$ reported by earlier authors. The neutrino cross section rises linearly with energy and with σ/E about 18% smaller than other measurements below 10 GeV. The average antineutrino slope at 55 GeV is consistent with measurements at low energy; however, a $(20 \pm 10)\%$ increase is indicated over our energy range.

The energy dependence of the neutrino and antineutrino total charged-current cross sections, $\nu_\mu (\bar{\nu}_\mu) + N \rightarrow \mu^- (\mu^+) + \text{hadrons}$, provides a fundamental test of two basic assumptions: (1) the four-fermion ($V-A$) weak interaction and (2) the scaling of the nucleon structure functions. These assumptions imply that the cross sections rise linearly with incident neutrino energy E and, hence, that the slope parameters $s = \sigma/E$ are independent of energy. Substantial failure of this test may signal deviations from the simplest local $V-A$ form, production of new hadronic or leptonic states, or qualitatively different behavior of the nucleon structure functions at high energies. It should be noted that small deviations from exact scaling are expected on theoretical grounds¹ and may have already been observed in electron and muon scattering.²

Measurements of the slope parameters at low energies³ ($E < 10$ GeV) give for neutrinos and antineutrinos respectively, $s = 0.74 \pm 0.05$ and $\bar{s} = 0.28 \pm 0.02$ in units of 10^{-38} cm²/GeV. Earlier direct measurements⁴ at high energies, while in agreement with these values, have rather large errors ($\sim 20\%$) and extend to only 110 GeV.

We present major new results on flux-normalized total cross sections in the energy range $45 < E < 205$ GeV, obtained with the Fermilab narrow-band beam⁵ and the California Institute of Technology-Fermilab neutrino detector.⁴ The total data sample consists of about 18 000 ν and 12 000 $\bar{\nu}$ interactions.

The incident neutrino flux is obtained directly from the measured number of pions and kaons in the decay region. These measurements have been described in a previous communication⁶; errors in the neutrino flux measurement are about 7%.

The neutrino target⁴ is a calorimeter consisting of 140 tons of steel plates interspersed with spark chambers (every 20 cm) and scintillation counters (every 10 cm). Hadron energies are determined by calorimetry. A steel toroidal spectrometer downstream of the target provides momentum analysis for muons.

Neutrino events were recorded when either or both of two independent triggers were satisfied. The first, the muon trigger (MT), required a secondary muon to traverse counters upstream and downstream of the toroidal magnet. No requirement was made on hadronic energy deposition. The second, the hadron trigger (HT), required a minimum energy deposition (≥ 6 GeV) in the target calorimeter along with a track that penetrated 150 cm of steel. The hadron trigger *did not involve the toroidal magnet*. By utilizing the substantial overlap of these two triggers, it was determined that the muon trigger efficiency was 97%, and the hadron trigger efficiency averaged 95%.

The measurement of total cross sections utilizing the narrow-band beam is in principle quite direct.⁴ Each of six beam settings⁶ yields two flux bands (ν_π, ν_K), from π and K decay, which

differ in mean energy by over a factor of 2 and with typical rms widths of 29% and 18%, respectively. The neutrino fluxes in the two energy bands are individually determined. Measurements of σ at the two energies are then obtained from the number of events induced by neutrinos in each of the bands.

For MT events, the ν_π , ν_K separation is made using the total observed neutrino energy (the sum of measured muon, E_μ , and hadron, E_h , energies) and the transverse vertex position. After correcting for azimuthal acceptance losses, these events provide a complete sample in the range of muon polar angles, $0 < \theta < \theta_1$ ($\theta_1 = 110$ mrad). The analysis of MT events is discussed in more detail in Ref. 6.

To complement this data sample, we utilize the HT events. Although these do not in general provide measured values of muon energy on an event-by-event basis, they do cover polar angles up to $\theta_2 = 360$ mrad with full efficiency (after correcting for azimuthal losses). The value of θ_2 results from the requirement that a charged particle traverse 150 cm of steel. This penetration cut insures that a muon is present.⁷

Without individually measured muon energies in the HT events, we utilize an alternative technique to separate the ν_π , ν_K data. This procedure is illustrated in Fig. 1 for one of the narrow-band beam settings (+190 GeV). The hadron energy distribution for all HT events is shown. Also plotted are the distributions for the ν_K MT events and the sum of the ν_π and ν_K MT events in restricted energy ranges. The angular coverage $\theta < \theta_1$ of the muon trigger implies, by kinematics, complete acceptance in hadron energy for $E_h < E_h^{\max}$, where E_h^{\max} depends on the incident neutrino energy.⁸ At any of the beam settings, E_h^{\max} for ν_K events is larger than the maximum possible hadron energy in ν_π events. The complete distribution for all ν_K events is obtained by combining the distribution from the muon trigger for $E_h < E_h^{\max}$ with that from the hadron trigger for $E_h > E_h^{\max}$. This distribution is indicated by the solid curve in the figure. The E_h distribution for ν_π events is obtained by subtracting the much smaller ν_K distribution from the total spectrum. The cross-hatched area in the figure yields the total number of ν_π events.⁹ Variations in the E_h^{\max} cuts by $\pm 10\%$ result in changes in the number of ν_π and ν_K events which are typically $< 3\%$.

The final separated E_h distributions do not contain events for $\theta > \theta_2$ (360 mrad). We estimate the

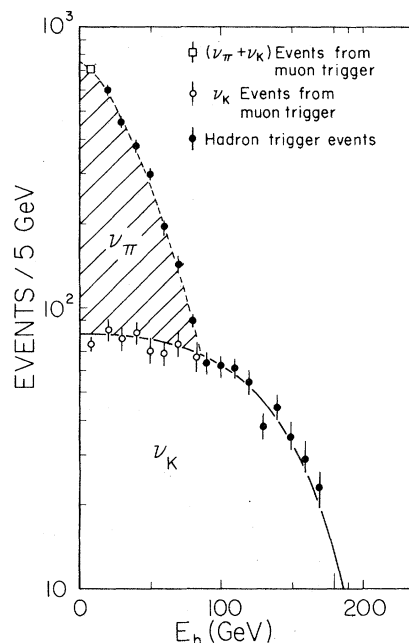


FIG. 1. The hadron energy distribution for events obtained at the +190-GeV beam setting. This figure illustrates the technique for separating events in the two energy bands ν_π and ν_K . All events have been corrected for azimuthal detection efficiency. Because the muon trigger for ν_K events has acceptance up to a hadron energy larger than the maximum possible E_h for ν_π events, the ν_K distribution is uniquely determined. The ν_π distribution (cross-hatched area) is obtained by subtracting the much smaller ν_K distribution from the total.

number of these missed events from the measured distributions in the scaled muon angle variable, $\kappa = 2M/E\theta^2$, for the separated ν_π , ν_K data. Here, the neutrino energy is obtained from the beam properties and the muon angle is measured for each event. By extrapolating these distributions to $\kappa = 0$, we determine corrections for this event loss that range from $(0 \pm 0.5)\%$ to $(6.6 \pm 2.5)\%$ for neutrinos and from $(0 \pm 0.5)\%$ to $(1.6 \pm 0.5)\%$ for antineutrinos, where the largest correction occurs at the lowest incident neutrino energies. The quoted errors reflect our uncertainties in making this correction and are incorporated into the total errors.

The resulting total cross sections represent integrals over the entire final-state phase space. The values and their errors are given in Table I and shown in Fig. 2. An overall normalization error of 4%, common to ν and $\bar{\nu}$, is not included in the errors shown. Our previously measured⁴ cross sections are consistent with these new

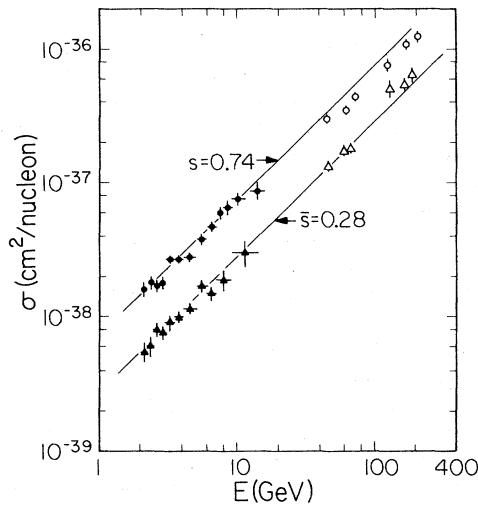


FIG. 2. Neutrino and antineutrino total cross sections as a function of the incident energy. Neutrino (circles) and antineutrino (triangles) data are shown from this experiment (open symbols) and from Ref. 3 (filled symbols). The errors on our data include all statistical and estimated systematic uncertainties, but not an overall 4% normalization uncertainty. For comparison, the best linear fits from Ref. 3 are shown.

measurements. The errors on these new data, however, are a factor of 5 smaller due to substantial improvements and redundancies in the technique.⁶ The best-fit slope parameters to the ν and $\bar{\nu}$ data (with all errors included) are

$$\langle s \rangle = (0.609 \pm 0.030) \times 10^{-38} \text{ cm}^2/\text{GeV}, \quad (1)$$

$$\langle \bar{s} \rangle = (0.290 \pm 0.015) \times 10^{-38} \text{ cm}^2/\text{GeV}. \quad (2)$$

TABLE I. Neutrino and antineutrino total charged-current cross sections at various incident energies. These values represent integrals over the entire phase space. All errors are included except an overall 4% calibration uncertainty common to all points. The quoted errors are dominantly from estimated systematic effects; in general, the raw statistical errors contribute less than half of the net error. Mean neutrino energies are known to 1.5%.

E (GeV)	σ^ν (10^{-38} cm^2)	E (GeV)	$\sigma^{\bar{\nu}}$ (10^{-38} cm^2)
45.2	30.1 ± 2.0	45.9	13.2 ± 0.7
61.3	35.3 ± 1.8	60.0	16.9 ± 0.8
72.4	44.4 ± 3.0	65.7	18.1 ± 1.1
125.0	76.3 ± 9.3	129.0	51.0 ± 7.4
171.0	109.2 ± 7.6	168.0	54.6 ± 5.7
205.0	122.4 ± 9.8	188.0	63.3 ± 8.6

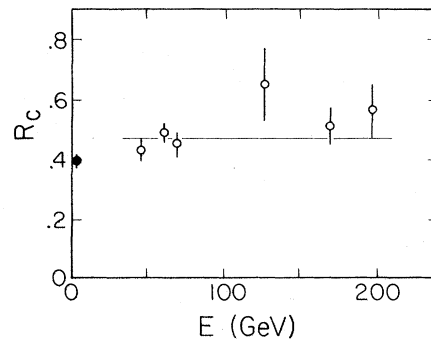


FIG. 3. The ratio of antineutrino to neutrino cross sections, $R_c = \bar{s}(E)/s(E)$, as a function of neutrino energy, E . The solid line indicates the best average. The higher-energy-data average is $(20 \pm 10)\%$ is higher than the lower-energy data. For comparison, the average value of this ratio from Ref. 3 is also shown (filled circle).

The neutrino data fit the hypothesis of linearity extremely well, with a $\chi^2 = 3.8$ for 5 degrees of freedom. The measured slope is about 18% (3.6 standard deviations) below¹⁰ the value quoted³ by experiments at low energy ($E < 10$ GeV). Small scaling violations as seen in μp and ep data² are a possible explanation¹ for this decrease at high energies.

The hypothesis of linearity fits the antineutrino data of Fig. 2 adequately with $\chi^2 = 6.5$ for 5 degrees of freedom although a systematic increase in \bar{s} at higher energies is indicated. The average slope $\langle \bar{s} \rangle$ is consistent with measurements at low energy.³

Figure 3 shows the ratio of antineutrino to neutrino cross sections $R_c = \bar{s}(E)/s(E)$ versus neutrino energy. The ratio of the average slopes is 0.476 ± 0.019 . We see no evidence for the dramatic and anomalous rise in this ratio observed by other authors¹¹ in the energy range 30 to 100 GeV. However, a more gentle increase of $(20 \pm 10)\%$ over our larger energy range (45 to 205 GeV) is indicated by the data.¹² This 2-standard-deviation effect is in contrast to a recent result¹³ in which no energy dependence was observed over the same energy range.

This work was supported by the U. S. Energy Research and Development Administration under Contract No. EY-76-C03-0068.

^(a) Present address: University of Rochester, Rochester, N. Y. 14627.

^(b) Present address: Northwestern University, Evan-

ston, Ill. 60201.

^(c) Present address: Fermi National Accelerator Laboratory, Batavia, Ill. 60510.

¹See M. Barnett and F. Martin, SLAC Report No. SLAC-PUB-1892, 1977 (unpublished); I. Karlziner and J. D. Sullivan, University of Illinois Report No. ILL-TH-77-18, 1977 (unpublished).

²See D. H. Perkins *et al.*, Phys. Lett. **67B**, 347 (1977), and references therein.

³D. H. Perkins, Rep. Prog. Phys. **40**, 409 (1977); T. Eichten *et al.*, Phys. Lett. **46B**, 274 (1973); D. H. Perkins, private communication.

⁴B. C. Barish *et al.*, Phys. Rev. Lett. **35**, 1316 (1975).

⁵B. C. Barish *et al.*, unpublished; P. Limon *et al.*, Nucl. Instrum. Methods **116**, 317 (1974).

⁶B. C. Barish *et al.*, Phys. Rev. Lett. **39**, 741 (1977).

⁷A smaller penetration requirement risks contamination by neutral-current interactions. See F. S. Merritt *et al.*, California Institute of Technology Report No. CALT 68-600, 1977 (to be published).

⁸ $E_h^{\max} = E/(1 + \kappa_1)$ with $\kappa_1 = 2M/E\theta_1^2$, M the nucleon (target) mass, and θ_1 the maximum muon angle sub-

tended.

⁹The spectra of events versus E_h can also be compared with mean neutrino energy, E , to determine $\langle y \rangle$. This will be the subject of a subsequent communication [B. C. Barish *et al.*, California Institute of Technology Report No. CALT 68-606 (to be published)].

¹⁰This difference could result from a 10-GeV boson propagator, but that hypothesis gives a bad fit to our data. Our data alone gives $M_w > 30$ GeV (90% confidence level) with no scale breaking. If a scale-breaking Q^2 dependence that lowers our sensitivity (e.g., $\langle Q^2/E \rangle \propto E^{-0.15}$) is allowed, our mass limit is $M_w > 20$ GeV.

¹¹A. Benvenuti *et al.*, Phys. Rev. Lett. **37**, 189 (1976).

¹²The quoted errors include all of our known uncertainties. An energy-dependent rise in the slope σ/E might result from mismeasurement of the $\pi/K/p$ ratios and/or misidentification of $\bar{\nu}_\pi$ - or $\bar{\nu}_K$ -induced events due to mismeasurement of the secondary muon. However, our measured $(1/E)d\sigma/dy$ at $y=0$ (see Ref. 6), which also depends on these effects, show no energy dependence.

¹³M. Holder *et al.*, Phys. Rev. Lett. **39**, 433 (1977).

Quantum Chromodynamics Predictions for the Associated Production of Charm by Neutrinos

H. Goldberg

Stanford University Accelerator Center, Stanford University, Stanford, California 94305, and
Department of Physics, Northeastern University, Boston, Massachusetts 02115^(a)

(Received 7 September 1977)

Cross sections for the inclusive production of charm-anticharm pairs in the hadron showers of neutrino scattering are calculated within framework of quantum chromodynamics. A branching ratio of less than 10^{-3} , insufficient to account for the like-sign dimuons observed by Barish *et al.*, Benvenuti *et al.*, and Holder *et al.* and trimuons observed by Barish *et al.* and Benvenuti *et al.*, is obtained for $\alpha_s = 0.4$ at values of x between 0.05 and 0.3, and $\nu \sim 50-75$ GeV.

Trimuons^{1,2} and like-sign dimuons³⁻⁵ have recently been observed in high-energy neutrino experiments. It has been proposed⁶ that the production and subsequent decay of new heavy leptons ($m \sim 10$ GeV) are responsible for these events. However, at least in the case of the like-sign dimuons, the events may be accounted for through the associated production of charm-anticharm pairs in (0.5-1)% of the hadron showers.^{4,7} Hence the heavy-lepton interpretation of the multimuon events must be measured against at least this alternative.

In a recent Letter, Bletzacker, Nieh, and Soni⁸ have presented a phenomenological model of $c\bar{c}$ pair production in the diffractive (small- x) region in order to account for the kinematic distributions of the multimuons. Since the publication of this work, however, a "large" sample of 47 $\mu^-\mu^-$ events has been reported⁵ in a ν -Fe ex-

periment by Holder *et al.* The background from π^- and K^- decay is estimated to contribute 30 ± 7 events, so that it is possible that there are 17 ± 7 $\mu^-\mu^-$ events of direct origin. The $\langle x_{\text{vis}} \rangle$ of all the events is 0.28, so that if there are events of direct origin, it is likely that they are *not* in the diffractive region. (The seven events reported in Ref. 3 also have $\langle x_{\text{vis}} \rangle \approx 0.2$.) In addition, the work of Ref. 8 does not provide a theoretical basis for the overall normalization of the cross section for the associated production of charmed hadrons.

Thus, it is of considerable practical interest to provide a theoretical model for inclusive charm-anticharm production in the nondiffractive ("normal x ") region of ν -nucleus scattering. Such a model, based on the standard SU(3) color gauge theory of the strong interactions (quantum chromodynamics, "QCD") is presented in this paper.